Bioorganic Chemistry 104 (2020) 104304

Contents lists available at ScienceDirect

Bioorganic Chemistry

journal homepage: www.elsevier.com/locate/bioorg

Structure-activity relationship studies of prostate-specific membrane antigen (PSMA) inhibitors derived from α-amino acid with (*S*)- or (*R*)-configuration at P1′ region

Hongmok Kwon [a], Hyunwoong Lim [a], Hyunsoo Ha [a], Doyoung Choi [a], Sang-Hyun Son [a], Hwanhee Nam [b,c], Il Minn [b,c], Youngjoo Byun [a,d,*]

[a] College of Pharmacy, Korea University, 2511 Sejong-ro, Sejong 30019, Republic of Korea
[b] Russell H. Morgan Department of Radiology and Radiological Science, Johns Hopkins Medical Institutions, Baltimore, MD 21287, United States
[c] Institute for NanoBioTechnology (INBT), Johns Hopkins University, 3400 N Charles St, Baltimore, MD 21218, United States
[d] Biomedical Research Center, Korea University Guro Hospital, 148 Gurodong-ro, Guro-gu, Seoul 08308, Republic of Korea

ARTICLE INFO

Keywords:
Absolute configuration
PSMA
SAR
Prostate cancer

ABSTRACT

Prostate-specific membrane antigen (PSMA), a type II membrane glycoprotein, is considered an excellent target for the diagnosis or treatment of prostate cancer. We previously investigated the effect of β- and γ-amino acids with (*S*)- or (*R*)-configuration in the S1 pocket on the binding affinity for PSMA. However, comprehensive studies on the effect of α-amino acid with (*R*)-configuration in the S1′ pocket has not been reported yet. We selected ZJ-43 (**1**) and DCIBzL (**5**) as templates and synthesized their analogues with (*S*)- or (*R*)-configuration in the *P*1 and *P*1′ regions. The PSMA-inhibitory activities of compounds with altered chirality in the *P*1′ region were dropped dramatically, with their IC_{50} values changing from nM to μM ranges. The compounds with (*S*)-configuration at both *P*1 and *P*1′ regions were more potent than the others. The findings of this study may provide insights regarding the structural modification of PSMA inhibitor in the S1′ binding pocket.

1. Introduction

Prostate-specific membrane antigen (PSMA), also known as glutamate carboxypeptidase II (GCPII), is a zinc metallopeptidase that hydrolyzes endogenous *N*-acetylaspartylglutamate (NAAG) to *N*-acetylaspartate (NAA) and glutamate [1,2]. PSMA exhibits restricted expression with an enzymatic active site in the extracellular region and on the cell surface of prostate cancer (PCa) cells, and its upregulated expression levels correlated with tumor progression and metastasis [3,4]. Thus, PSMA is considered one of the most attractive targets for the diagnosis of PCa [5]. In addition, since excessive production of glutamate causes glutamate-associated neurotoxicity and neuronal death, PSMA-mediated release of glutamate by cleavage of NAAG in the brain has been identified as a potential target for the regulation of intrasynaptic glutamate concentration [6–10]. The small molecules bearing functional groups including phosphinate, phosphoramidate, urea, hydroxamate, and thiol have been identified as key scaffolds of PSMA inhibitors [11–17]. Those scaffolds interact with Zn^{2+} at the active site [12,13,18–22]. Among them, urea scaffold has been in the limelight since the seminal work of Kozikowski and co-workers was first reported in 2001 [14]. ZJ-43 (**1**, Fig. 1), a representative compound of the urea-based PSMA inhibitors with high potency (K_i = 0.8 nM) [6], has been widely exploited as a template for development of PSMA inhibitors and is a prototype molecule for investigating the physiological features of PSMA. ZJ-43 treatment in various animal models substantiated that PSMA inhibition results in neuroprotection by regulating the glutamate levels, indicating a possibility for it to treat schizophrenia, traumatic brain injury, and neuropathic pain [23–25]. In addition, ZJ-43 also provided a structural prototype for the development of urea-based PSMA inhibitors [26,27]. Not only the synthetic accessibility and high potency of urea-based compounds, but also the chemical stability of urea group allowed various structural modifications. The versatile intermediate Lys-urea-Glu has been considered the most attractive template to develop imaging or therapeutic agents for PCa. For example, treatment with DCIBzL (**5**), one of the potent PSMA inhibitors (K_i = 0.01 nM), demonstrated that Lys-urea-Glu can be the most useful scaffold for developing PCa imaging agents including single photon emission computed tomography (SPECT), positron emission tomography (PET),

* Corresponding author at: College of Pharmacy, Korea University, 2511 Sejong-ro, Sejong 30019, Republic of Korea.
E-mail address: yjbyun1@korea.ac.kr (Y. Byun).

https://doi.org/10.1016/j.bioorg.2020.104304
Received 22 May 2020; Received in revised form 15 September 2020; Accepted 20 September 2020
Available online 24 September 2020

and optical scanning in animal models and clinical studies [28–30]. The *p*-iodobenzoyl group of DCIBzL interacts with the S1 hydrophobic accessory pocket, which consists of Arg463, Arg534, and Arg536, to contribute to the enhancement of PSMA-inhibitory activity [31]. Based on the structural freedom of S1 pocket, diverse functional groups have been conjugated to the *P*1 region of Lys-urea-Glu PSMA inhibitors, targeting the clinical application for PCa diagnosis and treatment [13,30,32–35].

While researching the structural modification of urea-based PSMA inhibitors, we recently reported structure–activity relationship (SAR) studies of PSMA inhibitors derived from β- and γ-amino acid analogues with (*S*)- or (*R*)-configuration at the S1 binding site [36]. The β- and γ-amino acid-derived compounds presented critical alterations in the PSMA-inhibitory activities depending on their absolute configuration at the *P*1 region. This result prompted us to investigate the effect of the absolute configuration in the *P*1′ region that interacts with the S1′ pharmacophore pocket and has not been sufficiently studied yet. Although Tsukamoto and colleagues reported carbamate-based compounds with (*S*)- or (*R*)-configuration at the S1 or S1′ binding sites derived from ZJ-43 [37], urea-based compounds with (*R*)-configuration at the *P*1′ region have not been studied comprehensively.

In this study, we synthesized and evaluated a small number of ZJ-43 and DCIBzL analogues to examine the effect of absolute configuration in the *P*1 and *P*1′ region of urea-based compounds on the PSMA-binding affinity. We selected ZJ-43 (**1**) to investigate the effect of configurational change in the S1′ site without affecting the S1 pocket much. We also selected DCIBzL (**5**) to determine the effect of chirality changes on the binding leverage of S1 and S1 accessory pocket.

2. Results and discussion

2.1. Synthesis of urea-based PSMA inhibitors

Compounds **1**–**4** were synthesized from commercial L- or D-glutamic acid di-*tert* butyl ester by attaching L- or D-leucine *tert*-butyl esters according to the synthetic routes described in Scheme 1. Compound **5** was also prepared by applying the reported procedure [28] whereas the other compounds (**6**–**8**) were synthesized by modifying the synthetic method used for synthesizing **5** [36], as shown in Scheme 2. Briefly, reaction of L- or D-glutamic acid di-*tert* butyl ester with triphosgene in the presence of triethylamine, followed by the addition of Leu or Lys, provided the Leu-urea-Glu (**9**–**12**) or Lys-urea-Glu compounds (**13**–**15**), respectively. The *tert*-butyl group of the urea compounds (**9**–**15**) were removed by adding 25% trifluoroacetic acid (TFA) in CH_2Cl_2. The deprotected Lys-urea-Glu compounds (**13**–**15**) without further purification were used for the reaction with *N*-succinimidyl 4-iodobenzoate to afford the final compounds **6**–**8**.

All final compounds were purified by semi-preparative reversed-phase high-performance liquid chromatography (RP-HPLC) with high purity (>95%) using acetonitrile (ACN) and water containing 0.1% formic acid (FA) as mobile phase. The chemical structure of the final compounds were analyzed by NMR spectroscopy and ESI-MS. We monitored all final compounds in two different eluent conditions (ACN/water and methanol/water) using analytical RP-HPLC to compare the differences in lipophilicity between isomers. As shown in Fig. 2, compounds **1** (*S*/*S*) and **4** (*R*/*R*) displayed faster retention time than their diastereomers **2** (*R*/*S*) and **3** (*S*/*R*) in ACN/water eluent condition. The compounds that are enantiomers (**1**/**4** and **2**/**3**) showed the same retention times in the HPLC experiment. These results were found to be consistent for compounds **5**–**8** irrespective of the mobile phase mixtures.

2.2. In vitro NAALADase assays

Fluorescence-based NAALADase assay [38,39] was applied to determine the PSMA-inhibitory activities of the prepared 8 compounds and the results are summarized in Table 1. Significant decreases in the PSMA-inhibitory activities of ZJ-43 (**1**, IC_{50} = 4.03 nM) and DCIBzL (**5**, IC_{50} = 0.13 nM) were observed when the (*S*)-configuration in the *P*1 region was changed to the (*R*)-configuration (**2**, IC_{50} = 197 nM; **6**, 1200 nM), which is consistent with the results reported previously [36,37]. Because of the bulky *p*-iodobenzoyl group at **6**, the effect of chirality change in the *P*1 region at **6** was greater than that of **2**. When the stereochemistry of glutamic acid at the *P*1′ region was changed from (*S*)- to (*R*)-configuration, compounds **3** (IC_{50} > 10 μM) and **7** (IC_{50} = 2410 nM) almost lost the PSMA-inhibitory activities. These results indicate that the S1′ site is much more sensitive for stereochemistry than the S1 site, which is in accordance with the argument that S1 site provides more structural freedom than the S1′ site [13]. Interestingly, compound **7** showed a little stronger PSMA-inhibitory activity than **3** because the interaction of the *p*-iodobenzoyl group with accessory hydrophobic pocket, which is formed by the arginine patch at the S1 accessary site, might offset the effect of the chirality change at the *P*1′ region. Both compounds **4** and **8** with (*R*/*R*) configurations at the *P*1 and *P*1′ sites displayed no PSMA-inhibitory activities, demonstrating that the α-amino acids with (*R*)-configuration in the urea-based PSMA inhibitors negatively affected the interaction with the key residues in both the S1

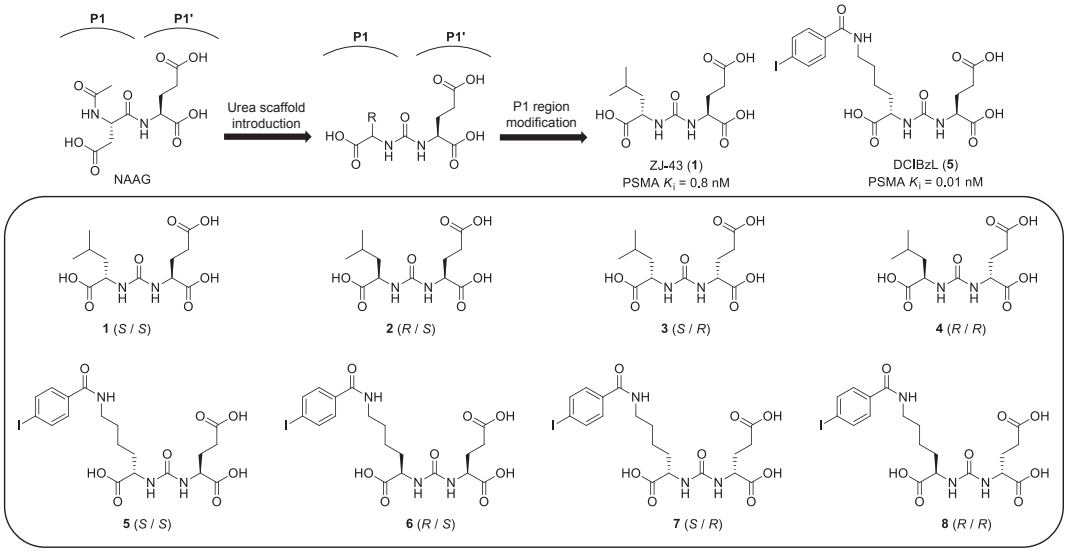

Fig. 1. Design concept of urea-based PSMA inhibitors derived from α-amino acids with (*S*)- or (*R*)-configuration.

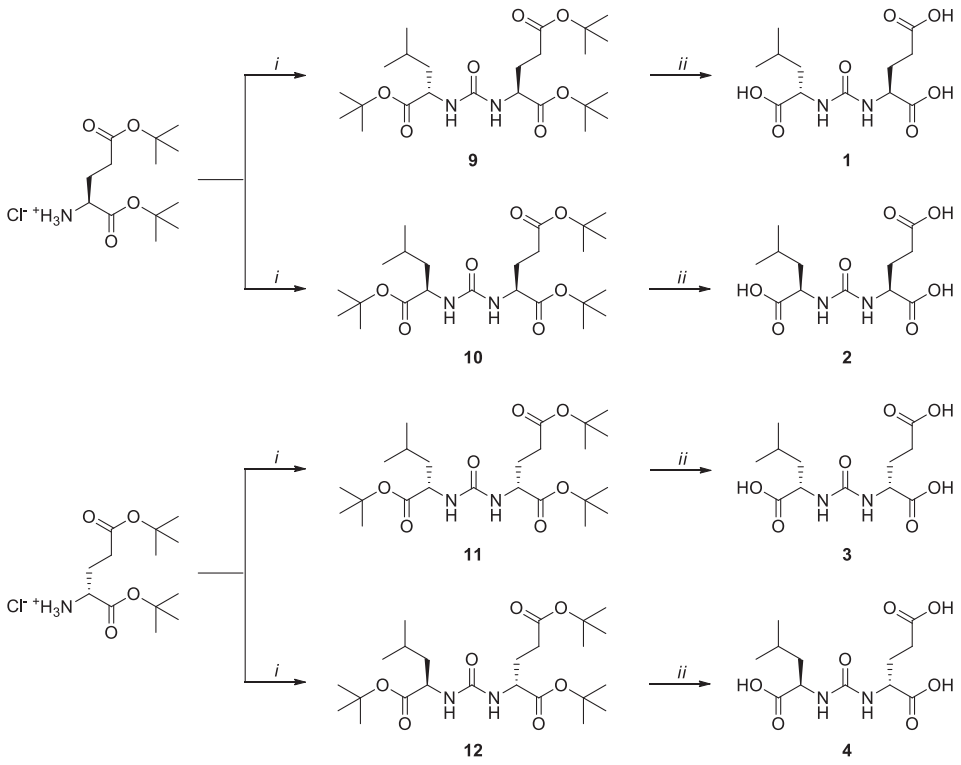

Scheme 1. Synthetic route for compounds **1**–**4**[a]. [a]Reagents and reaction conditions: (*i*) Triphosgene, L-Leu di-*tert* butyl ester HCl (for **9** and **11**) or D-Leu di-*tert* butyl ester HCl (for **10** and **12**), Et_3N, CH_2Cl_2, –78℃ to rt, 24 h; (*ii*) TFA/CH_2Cl_2 (1/4, v/v), rt, 3 h.

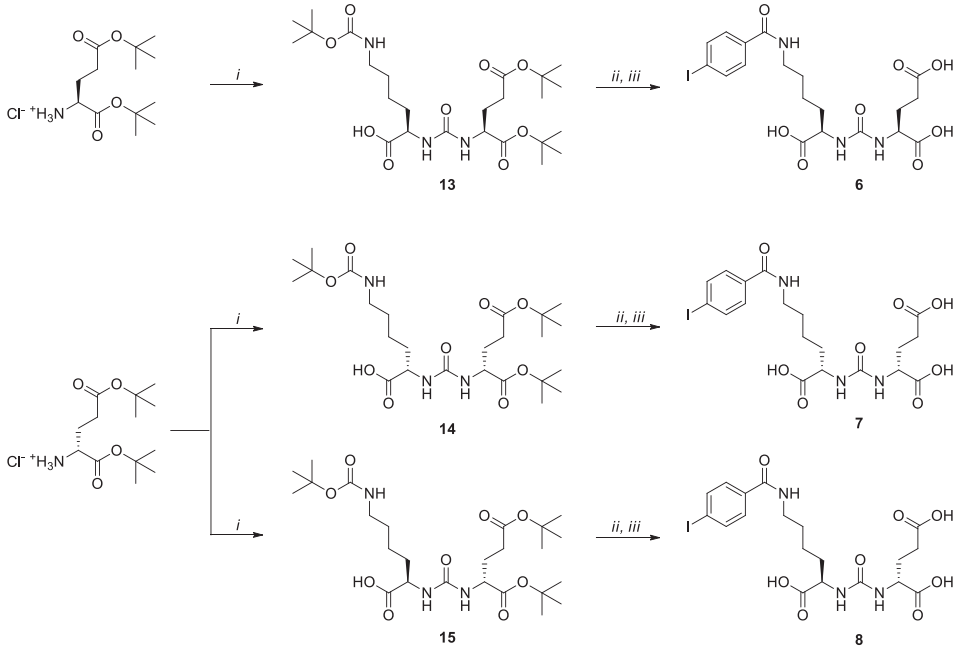

Scheme 2. Synthetic route for compounds **6**–**8**[a]. [a]Reagents and reaction conditions: (*i*) Triphosgene, N^{ε}-Boc-L-Lys (for **14**) or N^{ε}-Boc-D-Lys (for **13** and **15**), Et_3N, CH_2Cl_2, –78 ℃ to rt, 24 h; (*ii*) TFA/CH_2Cl_2 (1/4, v/v), rt, 3 h; (*iii*) *N*-succinimidyl 4-iodobenzoate, Et_3N, DMF, rt, 2.5 h.

and S1′ sites of PSMA.

2.3. Molecular modeling studies

To elucidate the binding modes of the synthesized compounds, *in silico* docking studies were conducted using Surflex-Dock Geom module using SYBYL-X 2.1.1 software (Tripos Inc, NJ). Compounds **1**–**4** were docked in the active site of the X-ray crystal structure of PSMA complexed with ZJ-43 (PDB ID: 6FE5) [37], whereas **5**–**8** were docked in the X-ray crystal structure of PSMA complexed with DCIBzL (PDB ID: 3D7H) [13]. Schematic depiction of the key interactions between the synthesized compounds and PSMA active site is provided in Supplementary data. Docking studies revealed that the chirality change in **1** forced the urea group away from Zn^{2+}, resulting in the loss of PSMA-inhibitory

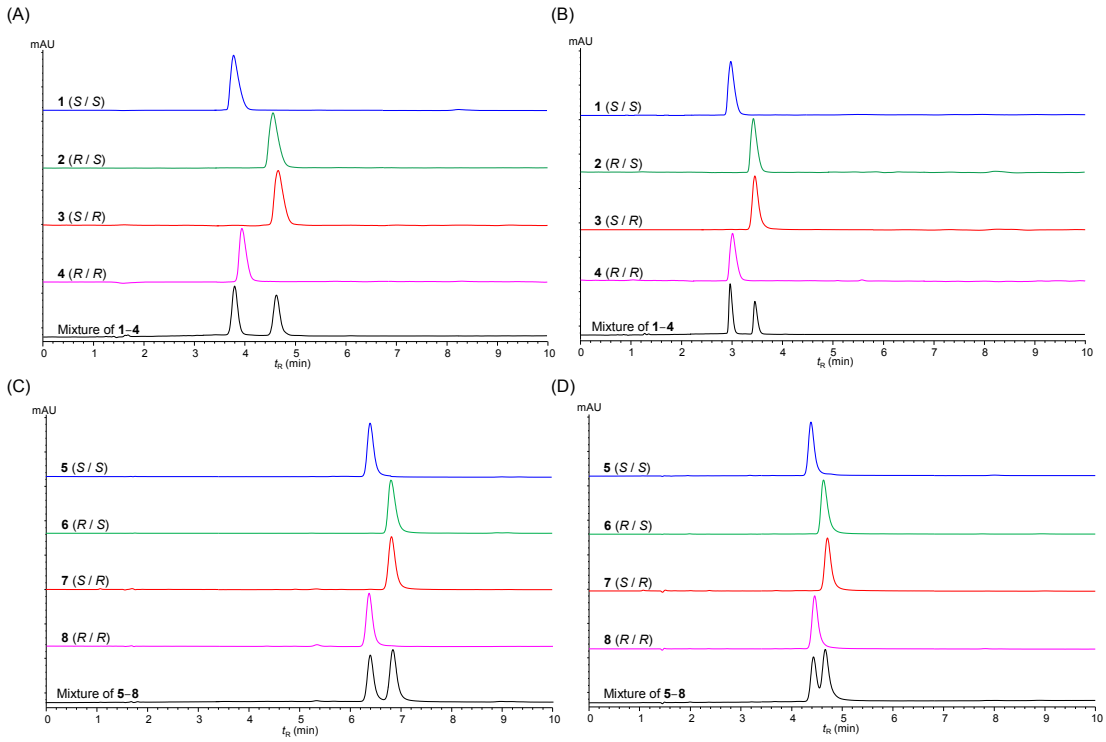

Fig. 2. (A) HPLC spectra of compounds **1**–**4** eluted with ACN and water (20:80, v/v, and 0.1% FA), flow rate: 1 mL/min. (B) HPLC spectra of compounds **1**–**4** eluted with methanol and water (50:50, v/v, and 0.1% FA), flow rate: 1 mL/min. (C) HPLC spectra of compounds **5**–**8** eluted with ACN and water (30:70, v/v, and 0.1% FA), flow rate: 1 mL/min. (D) HPLC spectra of compounds **5**–**8** eluted with methanol and water (60:40, v/v, and 0.1% FA), flow rate: 1 mL/min.

Table 1
In vitro PSMA-inhibitory activity of the synthesized compounds.

Compound	Stereochemistry	IC_{50} (nM)	95% CI[a]
ZJ-43 (1)	(*S*,*S*)	4.03	2.96–5.49
2	(*R*,*S*)	197	123–316
3	(*S*,*R*)	>10000	
4	(*R*,*R*)	>10000	
DCIBzL (5)	(*S*,*S*)	0.13	0.04–0.40
6	(*R*,*S*)	1200	529–2740
7	(*S*,*R*)	2410	1230–4730
8	(*R*,*R*)	>10000	

[a] Confidence interval.

activity (Table 2). Despite insignificant differences in binding poses between **2** and **3**, compound **3** showed longer distance of Zn^{2+} from oxygen of urea group than **2**. In addition, the γ-carboxylate group of glutamic acid of **3** was closer to Leu428 than that of **2**. Leu428 contributes nonpolar interactions to the inhibitor binding [13], which might have led to the repulsion of **3** to S1′ site. Compound **4** was docked in the active site of PSMA in a reverse pose contrary to **2** or **3**, which failed to present hydrogen bonding interaction with Sĺ pocket, particularly Lys699 (Fig. 3).

Because of distorted binding pose, **4** exhibited the longest distance (4.38 Å) of Zn^{2+} from oxygen of urea scaffold among **1**–**4**. Most of the potent urea-based or carbamate-based PSMA inhibitors exhibited interaction with Zn^{2+} within 2–3 Å range [13,32,37,40–42], providing an explanation for the diminished PSMA-inhibitory activity of ZJ-43 analogues. In docking simulation experiments of **5**–**8**, compounds **5** and **8** showed the highest (15.1531) and lowest (13.1755) *T*-scores, respectively, correlating with the *in vitro* assay results. The *p*-iodobenzoyl groups of **5**–**8** were projected into the S1 hydrophobic accessory pocket (Fig. 3). While compound **6** exhibited a shorter distance (1.99 Å) between oxygen of urea and Zn^{2+} than **5** (2.55 Å), it showed less hydrogen-bonding interactions with amino acids within a range of 2.50 Å than **5**. As the chirality of lysine was changed from (*S*) to (*R*), the carboxylate group in lysine of **6** was located at>2.50 Å range from Arg534, Arg536, and Asn519. The urea group of **7** was farther away from Zn^{2+} (5.58 Å) than **8** (4.18 Å) but the carboxylate of lysine presented a pose to interact with Zn^{2+}, whereas **8** displayed no interaction with Zn^{2+}. In addition, the urea group of **8** formed hydrogen bonds with Gly518 less tightly than **7**. Overall, the chirality changes in urea-based PSMA inhibitors in the α-amino acid region led not only to alterations in hydrogen bonding interaction with PSMA active site but also relocation of urea group from active site Zn^{2+}, resulting in detrimental effects on the PSMA-inhibitory activities.

Table 2
In silico docking data of synthesized compounds.

Cmpd	Stereo-chemistry	*T*-score	H-bonding amino acids[a]	Zn^{2+}–O of urea distance
ZJ-43 (1)	(*S*,*S*)	12.3131	R210, N257, G518, N519, R534, R536, Y552, K699, Y700[b]	2.88 Å[b]
2	(*R*,*S*)	11.4895	R210, N257, G518, N519, R534, Y552	3.19 Å
3	(*S*,*R*)	11.8887	R210, N257, G518, N519, R534, R536, Y552, K699	3.37 Å
4	(*R*,*R*)	11.0603	G518, N519, R534, Y552	4.38 Å
DCIBzL (5)	(*S*,*S*)	15.1531	R210, N257, E425, G518, N519, R534, R536, Y552, K699, Y700[c]	2.55 Å[c]
6	(*R*,*S*)	14.0610	R210, N257, R463, G518, Y552, K699	1.99 Å
7	(*S*,*R*)	13.3062	R210, E425, R463, G518, Y552, K699	5.58 Å
8	(*R*,*R*)	13.1755	R210, N257, G518, N519, R534, Y552	4.18 Å

[a] Amino acids within a range of 2.50 Å.
[b] Based on PSMA X-ray crystal structure in complex with **1** (PDB ID: 6FE5).
[c] Based on PSMA X-ray crystal structure in complex with **5** (PDB ID: 3D7H).

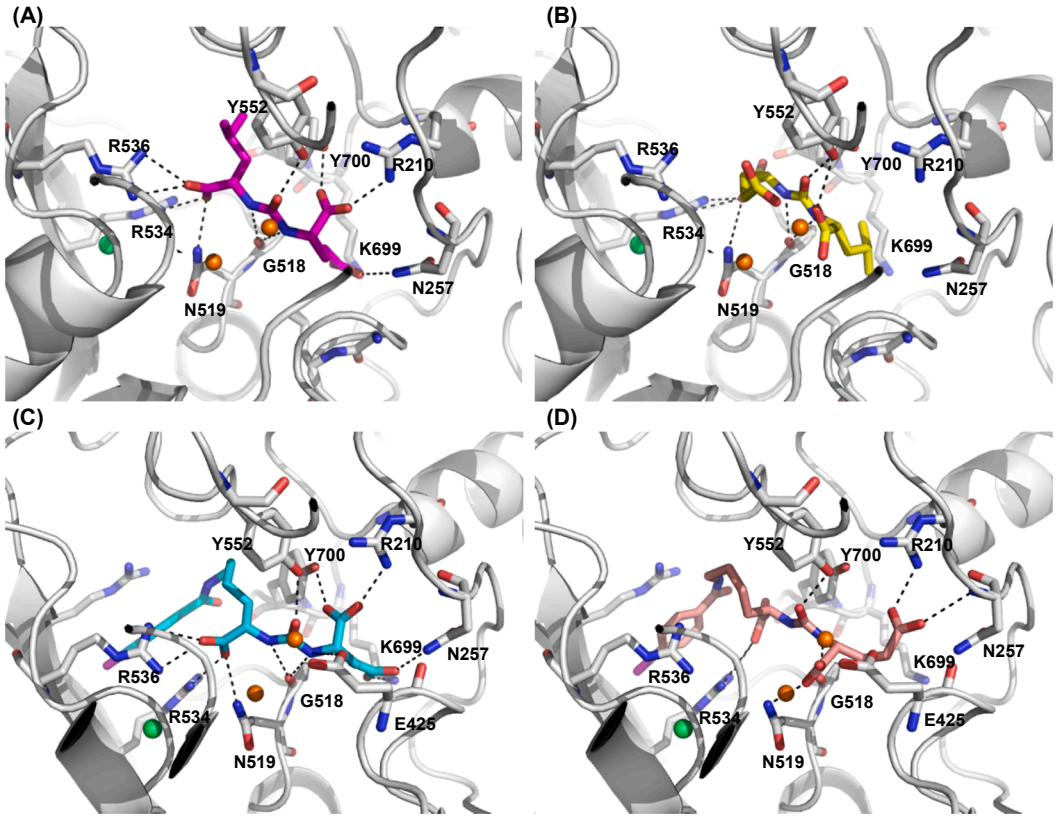

Fig. 3. (A) Bound-pose of ZJ-43 (**1**) in the active site of PSMA (PDB ID: 6FE5). (B) Docked-pose of **4** in the active site of PSMA. (C) Bound-pose of DCIBzL (**5**) in the active site of PSMA (PDB ID: 3D7H). (D) Docked-pose of **8** in the active site of PSMA. The active site zinc and chloride ions are shown as orange and lime green spheres, respectively. (For interpretation of the references to colour in this figure legend, the reader is referred to the web version of this article.)

3. Conclusion

In this study, we synthesized 8 compounds to investigate the absolute configuration of the PSMA inhibitors derived from α-amino acids and their effect on the PSMA-inhibitory activities. Two potent urea-based PSMA inhibitors, ZJ-43 (**1**) and DCIBzL (**5**), were used as molecular templates for introducing structural variations. The PSMA-inhibitory activities changed dramatically when changed from (*S*) to (*R*)-configuration, and thus substantiating α-amino acids with (*S*)-configuration are favorable for both the S1 and S1′ sites of PSMA. Particularly, the chirality change of glutamic acid moiety at the *P*1′ region affected the PSMA-inhibitory activity more than that of the *P*1 region, demonstrating that the S1′ site is a pharmacophore pocket. In molecular docking studies, the synthesized compounds with changed chirality showed distorted binding poses leading to the shifted position of urea group from Zn^{2+} at the PSMA active site. These results support previous studies showing that the S1′ pocket is structurally rigid and much less permissive than the S1 pocket [12,27,43]. However, despite relatively few reported cases compared to those of the *P*1 region, some studies have reported structural modifications of the *P*1′ region of PSMA inhibitors [26,27,44]. Especially, Yang and co-workers proved that there is still potential for structural optimization of the S1′ site binding [44]. The results of SARs in this study may provide insights for further modification of urea-based PSMA inhibitors.

4. Experimental section

4.1. General methods

All the chemicals and solvents used in the reaction were purchased from Sigma-Aldrich, TCI, or Alfa Aesar, and were used without further purification. Reactions were monitored by TLC on 0.25 mm Merck precoated silica gel plates (60 F_{254}). Reaction progress was monitored by TLC analysis using a UV lamp and/or $KMnO_4$ staining for detection purposes. Column chromatography was performed on silica gel (230–400 mesh, Merck, Darmstadt, Germany). ^1H and ^{13}C NMR spectra were recorded at room temperature (298 K) in $CDCl_3$ (7.26/77.16 ppm), CD_3CN (1.94/118.26 ppm), D_2O (4.79 ppm) or CD_3OD (3.31/49.00 ppm) on Bruker Ultrashield 600 MHz Plus spectrometer and referenced to an internal solvent. Chemical shifts are reported in parts per million (ppm). Coupling constants (*J*) are given in Hertz. Splitting patterns are indicated as s, singlet; d, doublet; t, triplet; q, quartet; m, multiplet; dd, double of doublet; br, broad for ^1H NMR data. High resolution mass spectra (HRMS) were recorded on an Agilent 6530 Accurate mass Q-TOF LC/MS spectrometer. High-performance liquid chromatography purification was performed on Agilent 1260 Infinity (Agilent). The purification of synthesized compounds was performed on a semi-preparative reverse-phase high-performance liquid chromatography (RP-HPLC; Agilent 1260 series HPLC instrument) using a semi-preparative column (Phenomenex Gemini-NX C18, 110 Å, 150 mm × 10 mm, 5 μm) using water (containing 0.1% FA) and acetonitrile (ACN; containing 0.1% FA) as mobile phase. UV detection was carried out at 220 nm. The purity of all final compounds was measured by analytical RP-HPLC on an Agilent 1260 Infinity (Agilent) with a C18 column (Phenomenex, 150 mm × 4.6 mm, 3 μm, 110 Å). RP-HPLC was performed on two different solvent systems of ACN/water or water/methanol. Purity of the tested compounds was > 95%.

4.2. Synthesis

4.2.1. *(S)-di-tert-butyl 2-(3-((S)-1-(tert-butoxy)-4-methyl-1-oxopentan-2-yl)ureido)pentanedioate (**9**).*

L-Glutamic acid di-*tert*-butyl ester hydrochloride (150 mg, 0.51 mmol) was dissolved in anhydrous dichloromethane (DCM, 3.0 mL)

then added triethylamine (0.57 mL, 4.08 mmol) under argon atmosphere. The solution was cooled to –78 ℃. To the reaction mixture was added dropwise triphosgene (47 mg, 0.16 mmol) dissolved in anhydrous DCM (1.5 mL). The reaction mixture was slowly warmed up to rt and stirred for 35 min. L-leucine *tert*-butyl ester hydrochloride (114 mg, 0.51 mmol) and triethylamine (0.57 mL, 4.08 mmol) dissolved in DCM (3.0 mL) were added in the reaction mixture and stirred at room temperature for 24 h. The organic layer was washed with water then drop the acidity level to pH 6 by 3 N HCl. The collected organic layer was dried over $MgSO_4$ then concentrated *in vacuo*. The residue was purified by flash column chromatography on silica gel with DCM–methanol (100:1 to 80:1, v/v) to afford compound **9** in 75% yield (181 mg, 0.38 mmol). ^{1}H NMR (600 MHz, CD_3OD): δ ppm 4.22–4.15 (m, 2H), 2.34–2.28 (m, 2H), 2.08–2.00 (m, 1H), 1.86–1.69 (m, 2H), 1.59–1.51 (m, 1H), 1.48–1.43 (m, 28H), 0.96 (d, J = 6.7 Hz, 3H), 0.93 (d, J = 6.5 Hz, 3H). ESI-HRMS (*m/z*): calculated for $C_{24}H_{45}N_2O_7^+$ $[M + H]^+$, 473.3221; found, 473.3231.

4.2.2. (S)-di-tert-butyl 2-(3-((R)-1-(tert-butoxy)-4-methyl-1-oxopentan-2-yl)ureido)pentanedioate (**10**).

This compound was afforded in 78% yield, following the same procedure described for synthesis of compound **9** with D-leucine *tert*-butyl ester HCl. ^{1}H NMR (600 MHz, $CDCl_3$): δ ppm 5.36–5.24 (m, 2H), 4.39–4.26 (m, 2H), 2.41–2.24 (m, 2H), 2.12–2.02 (m, 1H), 1.92–1.82 (m, 1H), 1.76–1.67 (m, 1H), 1.61–1.54 (m, 1H), 1.47–1.41 (m, 28H), 0.94 (d, J = 6.6 Hz, 6H). ESI-HRMS (*m/z*): calculated for $C_{24}H_{45}N_2O_7^+$ $[M + H]^+$, 473.3221; found, 473.3215.

4.2.3. (R)-di-tert-butyl 2-(3-((S)-1-(tert-butoxy)-4-methyl-1-oxopentan-2-yl)ureido)pentanedioate (**11**).

This compound was afforded in 65% yield, following the same procedure described for synthesis of compound **9** with D-glutamic acid di-*tert* butyl ester hydrochloride. ^{1}H NMR (600 MHz, $CDCl_3$): δ ppm 5.35–5.22 (m, 2H), 4.40–4.25 (m, 2H), 2.40–2.23 (m, 3H), 2.11–2.03 (m, 1H), 1.93–1.67 (m, 2H), 1.62–1.52 (m, 1H), 1.48–1.41 (m, 27H), 0.94 (d, J = 6.6 Hz, 6H). ESI-HRMS (*m/z*): calculated for $C_{24}H_{45}N_2O_7^+$ $[M + H]^+$, 473.3221; found, 473.3202.

4.2.4. (R)-di-tert-butyl 2-(3-((R)-1-(tert-butoxy)-4-methyl-1-oxopentan-2-yl)ureido)pentanedioate (**12**).

This compound was afforded in 78% yield, following the same procedure described for synthesis of compound **9** with D-glutamic acid di-*tert* butyl ester hydrochloride and D-leucine *tert* butyl ester hydrochloride. ^{1}H NMR (600 MHz, $CDCl_3$): δ ppm 5.02–4.72 (m, 2H), 4.37–4.30 (m, 2H), 2.38–2.23 (m, 3H), 2.11–2.03 (m, 1H), 1.90–1.82 (m, 1H), 1.75–1.66 (m, 1H), 1.60–1.52 (m, 1H), 1.55–1.41 (m, 27H), 0.94 (dd, J = 2.0 and 6.5 Hz, 6H). ESI-HRMS (*m/z*): calculated for $C_{24}H_{45}N_2O_7^+$ $[M + H]^+$, 473.3221; found, 473.3232.

4.2.5. (S)-2-(3-((S)-1-carboxy-3-methylbutyl)ureido)pentanedioic acid (**1**).

To a solution of compound **9** (181 mg, 0.38 mmol) in anhydrous DCM (6.0 mL) was added TFA (1.5 mL) at 0 ℃. The reaction mixture was stirred at room temperature for 3 h then concentrated *in vacuo*. The residue was purified with semi-preparative RP-HPLC using 0.1% FA in water and 0.1% FA in ACN as mobile phase. The product was afforded as colorless solid in 39% yield (45 mg, 0.15 mmol). ^{1}H NMR (600 MHz, D_2O): δ ppm 4.23 (dd, J = 5.2 and 9.2 Hz, 1H), 4.19 (t, J = 7.2 Hz, 1H), 2.47 (t, J = 7.3 Hz, 2H), 2.18–2.02 (m, 1H), 1.98–1.89 (m, 1H), 1.71–1.62 (m, 1H), 1.59 (t, J = 7.1 Hz, 2H), 0.90 (d, J = 6.6 Hz, 3H), 0.86 (d, J = 6.5 Hz, 3H). ^{13}C NMR (150 MHz, D_2O): δ ppm 179.26, 178.60, 177.62, 160.68, 53.94, 53.29, 41.21, 31.40, 27.62, 25.73, 23.55, 21.98. ESI-HRMS (*m/z*): calculated for $C_{12}H_{21}N_2O_7^+$ $[M + H]^+$, 305.1343; found, 305.1336.

4.2.6. (S)-2-(3-((R)-1-carboxy-3-methylbutyl)ureido)pentanedioic acid (**2**).

This compound was afforded in 44% yield, following the same procedure described for synthesis of compound **1** with compound **10**. ^{1}H NMR (600 MHz, D_2O): δ ppm 4.26 (dd, J = 5.0 and 9.2 Hz, 1H), 4.21 (t, J = 7.6 Hz, 1H), 2.49–2.43 (m, 2H), 2.20–2.11 (m, 1H), 1.99–1.90 (m, 1H), 1.71–1.62 (m, 1H), 1.59 (t, J = 7.6 Hz, 2H), 0.90 (d, J = 6.5 Hz, 3H), 0.87 (d, J = 6.5 Hz, 3H). ^{13}C NMR (150 MHz, D_2O): δ ppm 179.23, 178.58, 177.59, 160.57, 53.91 53.26 41.27 31.41 27.68, 25.76 23.57, 21.97. ESI-HRMS (*m/z*): calculated for $C_{12}H_{21}N_2O_7^+$ $[M + H]^+$, 305.1343; found, 305.1360.

4.2.7. (R)-2-(3-((S)-1-carboxy-3-methylbutyl)ureido)pentanedioic acid (**3**).

This compound was afforded in 52% yield, following the same procedure described for synthesis of compound **1** with compound **11**. ^{1}H NMR (600 MHz, D_2O): δ ppm 4.27 (dd, J = 5.1 and 9.2 Hz, 1H), 4.22 (t, J = 7.6 Hz, 1H), 2.52–2.44 (m, 2H), 2.21–2.12 (m, 1H), 2.00–1.91 (m, 1H), 1.72–1.63 (m, 1H), 1.60 (t, J = 7.1 Hz, 2H), 0.91 (d, J = 6.5 Hz, 3H), 0.88 (d, J = 6.5 Hz, 3H). ^{13}C NMR (150 MHz, D_2O): δ ppm 179.26, 178.61, 177.62, 160.60, 53.92, 53.27, 41.26, 31.42, 27.68, 25.77, 23.57, 21.96. ESI-HRMS (*m/z*): calculated for $C_{12}H_{21}N_2O_7^+$ $[M + H]^+$, 305.1343; found, 305.1354.

4.2.8. (R)-2-(3-((R)-1-carboxy-3-methylbutyl)ureido)pentanedioic acid (**4**).

This compound was afforded in 51% yield, following the same procedure described for synthesis of compound **1** with compound **12**. ^{1}H NMR (600 MHz, D_2O): δ ppm 4.25 (dd, J = 5.2 and 9.2 Hz, 1H), 4.21 (t, J = 7.2 Hz, 1H), 2.50 (t, J = 7.3 Hz, 2H), 2.20–2.12 (m, 1H), 2.00–1.91 (m, 1H), 1.73–1.65 (m, 1H), 1.61 (t, J = 7.1 Hz, 2H), 0.92 (d, J = 6.6 Hz, 3H), 0.88 (d, J = 6.5 Hz, 3H). ^{13}C NMR (150 MHz, D_2O): δ ppm 179.31, 178.65, 177.67, 160.72, 53.97, 53.31, 41.21, 31.42, 27.61, 25.74, 23.56, 21.97. ESI-HRMS (*m/z*): calculated for $C_{12}H_{21}N_2O_7^+$ $[M + H]^+$, 305.1343; found, 305.1353.

4.2.9. (R)-6-((tert-butoxycarbonyl)amino)-2-(3-((S)-1,5-di-tert-butoxy-1,5-dioxopentan-2-yl)ureido)hexanoic acid (**14**).

D-Glutamic acid di-*tert*-butyl ester hydrochloride (300 mg, 1.01 mmol) was dissolved in anhydrous DCM (5.0 mL) then added triethylamine (1.13 mL, 8.08 mmol) under argon atmosphere. The solution was cooled to –78 ℃. To the reaction mixture was added dropwise triphosgene (95 mg, 0.32 mmol) dissolved in anhydrous DCM (3.0 mL). The reaction mixture was slowly warmed up to rt and stirred for 35 min. N^{ε}-Boc-L-Lys (200 mg, 0.81 mmol) and trimethylamine (0.90 mL, 6.48 mmol) dissolved in DCM (8.0 mL) were added in the reaction mixture and stirred at room temperature for 24 h. The organic layer was washed with water then drop the acidity level to pH 6 by 3 N HCl. The collected organic layer was dried over $MgSO_4$ then concentrated *in vacuo*. The residue was purified by flash column chromatography on silica gel with DCM–methanol (100:1 to 10:1, v/v) to afford compound **14** in 49% yield. ^{1}H NMR (600 MHz, $(CD_3)_2SO$): δ ppm 4.05–3.97 (m, 1H), 3.90–3.80 (m, 1H), 2.85 (q, J = 6.6 Hz, 2H), 2.30–2.12 (m, 2H), 1.88–1.77 (m, 1H), 1.71–1.56 (m, 2H), 1.52–1.44 (m, 1H), 1.39 (s, 18H), 1.36 (s, 9H), 1.34–1.29 (m, 2H), 1.26–1.16 (m, 2H). ESI-HRMS (*m/z*): calculated for $C_{25}H_{45}N_3O_9Na^+$ $[M + Na]^+$, 554.3048; found, 554.3075.

4.2.10. (R)-6-((tert-butoxycarbonyl)amino)-2-(3-((R)-1,5-di-tert-butoxy-1,5-dioxopentan-2-yl)ureido)hexanoic acid (**15**).

This compound was afforded in 53% yield, following the same procedure described for synthesis of compound **14** with N^{ε}-Boc-D-Lys. ^{1}H NMR (600 MHz, $(CD_3)_2SO$): δ ppm 4.02–3.95 (m, 1H), 3.82 (brs, 1H), 2.84 (q, J = 6.2 Hz, 2H), 2.30–2.14 (m, 2H), 1.86–1.78 (m, 1H), 1.71–1.56 (m, 2H), 1.52–1.44 (m, 1H), 1.39 (s, 18H), 1.36 (s, 9H), 1.34–1.29 (m, 2H), 1.23–1.16 (m, 2H). ESI-HRMS (*m/z*): calculated for $C_{25}H_{45}N_3O_9Na^+$ $[M + Na]^+$, 554.3048; found, 554.3038.

4.2.11. (R)-2-(3-((S)-1-carboxy-5-(4-iodobenzamido)pentyl)ureido) pentanedioic acid (7).

To a solution of compound **14** (207 mg, 0.39 mmol) in anhydrous DCM (8.0 mL) was added TFA (2 mL) at 0 ℃. The reaction mixture was stirred at room temperature for 3 h and was concentrated *in vacuo*. Methanol added to the residue then was evaporated, and this procedure was conducted several times to remove residual TFA. Without further purification, the residue was dissolved in anhydrous *N*,*N*-dimethylformamide (DMF, 2.0 mL). *N*-Succinimidyl 4-iodobenzoate (160 mg, 0.47 mmol) and trimethylamine (0.43 mL, 3.12 mmol) was added to the reaction mixture under argon atmosphere. The reaction mixture was stirred at room temperature for 2.5 h and purified with semi-preparative RP-HPLC using 0.1% FA in water and 0.1% FA in ACN as mobile phase. The product was afforded as white solid in 22% yield (47 mg, 0.08 mmol). ^{1}H NMR (600 MHz, $CD_3CN/D_2O = 1/1$, v/v): δ ppm 8.41–8.34 (m, 2H), 8.05 (d, $J = 8.3$ Hz, 2H), 4.65 (brs, 2H), 3.84 (t, $J = 6.6$ Hz, 2H), 2.87 (brs, 2H), 2.62–2.51 (m, 1H), 2.41–2.59 (m, 2H), 2.23–2.01 (m, 3H), 1.97–1.85 (m, 2H). ^{13}C NMR (150 MHz, $CD_3CN/D_2O = 1/1$, v/v): δ ppm 177.52, 177.07, 169.38, 159.65, 138.90, 134.88, 130.01, 99.19, 55.18, 54.78, 40.64, 32.50, 31.60, 29.38, 28.39, 23.70. ESI-HRMS (*m/z*): calculated for $C_{19}H_{24}IN_3O_8Na^+$ $[M + Na]^+$, 572.0500; found, 572.0486.

4.2.12. (R)-2-(3-((R)-1-carboxy-5-(4-iodobenzamido)pentyl)ureido) pentanedioic acid (8).

This compound was afforded in 36% yield, following the same procedure described for synthesis of compound **7**. ^{1}H NMR (600 MHz, $CD_3CN/D_2O = 1/1$, v/v): δ ppm 8.37 (d, $J = 8.4$ Hz, 2H), 8.04 (d, $J = 8.2$ Hz, 2H), 4.73–4.62 (m, 2H), 3.83 (t, $J = 7.0$ Hz, 2H), 2.92 (t, $J = 7.7$ Hz, 2H), 2.64–2.54 (m, 1H), 2.44–2.35 (m, 1H), 2.35–2.26 (m, 1H), 2.23–2.15 (m, 1H), 2.14–2.04 (m, 2H), 1.97–1.87 (m, 2H). ^{13}C NMR (150 MHz, $CD_3CN/D_2O = 1/1$, v/v): δ ppm 177.38, 176.65, 169.37, 159.74, 138.90, 134.88, 130.02, 99.20, 54.50, 53.99, 40.63, 32.29, 31.31, 29.38, 28.04, 23.68. ESI-HRMS (*m/z*): calculated for $C_{19}H_{24}IN_3O_8Na^+$ $[M + Na]^+$, 572.0500; found, 572.0489.

N-succinimidyl *p*-iodobenzoate [45] and the compounds **5** [28], **13**, and **6** [36] were prepared as previously reported.

4.3. In vitro NAALADase assay

PSMA inhibitory activity of the final compounds was determined using a fluorescence-based assay according to a previously reported procedure [38,39]. LNCaP cell extracts were prepared by disrupting cell membrane sonication in Tris buffer (50 mM Tris [pH 7.4] and 0.5% Triton X-100). The cell lysates of LNCaP cell extracts were incubated with the synthesized compounds in the presence of 1 μM *N*-acetylaspartylglutamate. The amount of reduced glutamate was measured using the Amplex Red glutamic acid kit (Molecular Probes Inc., Eugene, OR). The fluorescence was measured with a Cytation 5 Image Reader (BioTek Instruments Inc., Winooski VT) with excitation at 545 nm and emission at 590 nm. Assays were performed in triplicate. Data analysis was performed using GraphPad Prism 7.0 (GraphPad Software, San Diego, CA). Inhibition curves were determined using the sigmoidal dose–response plots, and IC_{50} values were determined at the concentration at which enzyme activity was inhibited by 50%. Statistical significance was determined by 95% confidence interval on GraphPad Prism.

4.4. In silico docking studies

Ligand preparation and optimization: All peptide ligands were generated as 2D and 3D structure by *ChemDrawUltra* (ver. 12.0.2) and *Chem3D Pro* (ver. 11.0.1), respectively. The group of ligands were saved as *.sdf* file. Ligand preparation and optimization was performed by *'Sanitize'* preparation protocol in *SYBYL-X 2.1.1* (Tripos Inc., NJ) to clean up of the structures involving filling valences, standardizing, removing duplicates and producing only one molecule per input structure.

Protein preparation: The protein structures of in PDB format were downloaded from RCSB protein data bank (PDB ID: 6FE5 for compounds **1**–**4**, 3D7H for compounds **5**–**8**). Structure preparation tool in *SYBYL-X* 2.1.1 was employed for protein preparation. Water molecules of crystal structures were removed then conflicted side chains of amino acid residues were fixed. Hydrogen atoms were added under the application of *TRIPOS* Force Field as a default setting. Minimization process was performed by *POWELL* method, initial optimization option and termination gradient were set to *None* and 0.5 *kcal/(mol*Å)*, respectively.

The docking studies of all prepared ligands were performed by *Surflex-Dock Geom* module in *SYBYL-X 2.1.1*. Docking was guided by the *Surflex-Dock* protomol, an idealized representation of a ligand that makes every potential interaction with the binding site. Two factors related with a generation of Protomol are *Bloat(Å)* and *Threshold* were set to 0.5 and 0, respectively. Other parameters were applied with its default settings in all runs.

Declaration of Competing Interest

The authors declare no conflict of interests.

Acknowledgements

This work was supported by the National Research Foundation of Korea (2019R1A6A1A03031807 and 2020R1A2C2005919 to Y.B.).

Appendix A. Supplementary material

Supplementary data to this article can be found online at https://doi.org/10.1016/j.bioorg.2020.104304.

References

[1] R.E. Carter, A.R. Feldman, J.T. Coyle, Prostate-specific membrane antigen is a hydrolase with substrate and pharmacologic characteristics of a neuropeptidase, Proc. Natl. Acad. Sci. USA 93 (1996) 749–753.
[2] C. Barinka, C. Rojas, B. Slusher, M. Pomper, Glutamate carboxypeptidase II in diagnosis and treatment of neurologic disorders and prostate cancer, Curr. Med. Chem. 19 (2012) 856–870.
[3] A. Ghosh, W.D. Heston, Tumor target prostate specific membrane antigen (PSMA) and its regulation in prostate cancer, J. Cell. Biochem. 91 (2004) 528–539.
[4] D.A. Silver, I. Pellicer, W.R. Fair, W.D. Heston, C. Cordon-Cardo, Prostate-specific membrane antigen expression in normal and malignant human tissues, Clin. Cancer Res. 3 (1997) 81–85.
[5] A.K. Rajasekaran, G. Anilkumar, J.J. Christiansen, Is prostate-specific membrane antigen a multifunctional protein? Am. J. Physiol. Cell. Physiol. 288 (2005) C975–C981.
[6] R.T. Olszewski, N. Bukhari, J. Zhou, A.P. Kozikowski, J.T. Wroblewski, S. Shamimi-Noori, B. Wroblewska, T. Bzdega, S. Vicini, F.B. Barton, J.H. Neale, NAAG peptidase inhibition reduces locomotor activity and some stereotypes in the PCP model of schizophrenia via group II mGluR, J. Neurochem. 89 (2004) 876–885.
[7] D.J. Bacich, K.M. Wozniak, X.C. Lu, D.S. O'Keefe, N. Callizot, W.D. Heston, B. S. Slusher, Mice lacking glutamate carboxypeptidase II are protected from peripheral neuropathy and ischemic brain injury, J. Neurochem. 95 (2005) 314–323.
[8] J.H. Neale, R.T. Olszewski, L.M. Gehl, B. Wroblewska, T. Bzdega, The neurotransmitter N-acetylaspartylglutamate in models of pain, ALS, diabetic neuropathy, CNS injury and schizophrenia, Trends. Pharmacol. Sci. 26 (2005) 477–484.
[9] G.D. Ghadge, B.S. Slusher, A. Bodner, M.D. Canto, K. Wozniak, A.G. Thomas, C. Rojas, T. Tsukamoto, P. Majer, R.J. Miller, A.L. Monti, R.P. Roos, Glutamate carboxypeptidase II inhibition protects motor neurons from death in familial amyotrophic lateral sclerosis models, Proc. Natl. Acad. Sci. U. S. A. 100 (2003) 9554–9559.
[10] J. Zhou, J.H. Neale, M.G. Pomper, A.P. Kozikowski, NAAG peptidase inhibitors and their potential for diagnosis and therapy, Nat. Rev. Drug Discov. 4 (2005) 1015–1026.
[11] P.F. Jackson, D.C. Cole, B.S. Slusher, S.L. Stetz, L.E. Ross, B.A. Donzanti, D. A. Trainor, Design, synthesis, and biological activity of a potent inhibitor of the neuropeptidase N-acetylated alpha-linked acidic dipeptidase, J. Med. Chem. 39 (1996) 619–622.
[12] P.F. Jackson, K.L. Tays, K.M. Maclin, Y.S. Ko, W. Li, D. Vitharana, T. Tsukamoto, D. Stoermer, X.C. Lu, K. Wozniak, B.S. Slusher, Design and pharmacological activity of phosphinic acid based NAALADase inhibitors, J. Med. Chem. 44 (2001) 4170–4175.

[13] C. Barinka, Y. Byun, C.L. Dusich, S.R. Banerjee, Y. Chen, M. Castanares, A. P. Kozikowski, R.C. Mease, M.G. Pomper, J. Lubkowski, Interactions between human glutamate carboxypeptidase II and urea-based inhibitors: structural characterization, J. Med. Chem. 51 (2008) 7737–7743.
[14] A.P. Kozikowski, F. Nan, P. Conti, J. Zhang, E. Ramadan, T. Bzdega, B. Wroblewska, J.H. Neale, S. Pshenichkin, J.T. Wroblewski, Design of remarkably simple, yet potent urea-based inhibitors of glutamate carboxypeptidase II (NAALADase), J. Med. Chem. 44 (2001) 298–301.
[15] P. Majer, P.F. Jackson, G. Delahanty, B.S. Grella, Y.S. Ko, W. Li, Q. Liu, K. M. Maclin, J. Polakova, K.A. Shaffer, D. Stoermer, D. Vitharana, E.Y. Wang, A. Zakrzewski, C. Rojas, B.S. Slusher, K.M. Wozniak, E. Burak, T. Limsakun, T. Tsukamoto, Synthesis and biological evaluation of thiol-based inhibitors of glutamate carboxypeptidase II: discovery of an orally active GCP II inhibitor, J. Med. Chem. 46 (2003) 1989–1996.
[16] D. Stoermer, D. Vitharana, N. Hin, G. Delahanty, B. Duvall, D.V. Ferraris, B. S. Grella, R. Hoover, C. Rojas, M.K. Shanholtz, K.P. Smith, M. Stathis, Y. Wu, K. M. Wozniak, B.S. Slusher, T. Tsukamoto, Design, synthesis, and pharmacological evaluation of glutamate carboxypeptidase II (GCPII) inhibitors based on thioalkylbenzoic acid scaffolds, J. Med. Chem. 55 (2012) 5922–5932.
[17] D. Stoermer, Q. Liu, M.R. Hall, J.M. Flanary, A.G. Thomas, C. Rojas, B.S. Slusher, T. Tsukamoto, Synthesis and biological evaluation of hydroxamate-Based inhibitors of glutamate carboxypeptidase II, Bioorg. Med. Chem. Lett. 13 (2003) 2097–2100.
[18] J.R. Mesters, C. Barinka, W. Li, T. Tsukamoto, P. Majer, B.S. Slusher, J. Konvalinka, R. Hilgenfeld, Structure of glutamate carboxypeptidase II, a drug target in neuronal damage and prostate cancer, EMBO J. 25 (2006) 1375–1384.
[19] C. Barinka, M. Rovenska, P. Mlcochova, K. Hlouchova, A. Plechanovova, P. Majer, T. Tsukamoto, B.S. Slusher, J. Konvalinka, J. Lubkowski, Structural insight into the pharmacophore pocket of human glutamate carboxypeptidase II, J. Med. Chem. 50 (2007) 3267–3273.
[20] M. Navratil, J. Ptacek, P. Sacha, J. Starkova, J. Lubkowski, C. Barinka, J. Konvalinka, Structural and biochemical characterization of the folyl-poly-gamma-l-glutamate hydrolyzing activity of human glutamate carboxypeptidase II, FEBS J. 281 (2014) 3228–3242.
[21] Z. Novakova, J. Cerny, C.J. Choy, J.R. Nedrow, J.K. Choi, J. Lubkowski, C. E. Berkman, C. Barinka, Design of composite inhibitors targeting glutamate carboxypeptidase II: the importance of effector functionalities, FEBS J. 283 (2016) 130–143.
[22] Z. Novakova, K. Wozniak, A. Jancarik, R. Rais, Y. Wu, J. Pavlicek, D. Ferraris, B. Havlinova, J. Ptacek, J. Vavra, N. Hin, C. Rojas, P. Majer, B.S. Slusher, T. Tsukamoto, C. Barinka, Unprecedented Binding Mode of Hydroxamate-Based Inhibitors of Glutamate Carboxypeptidase II: Structural Characterization and Biological Activity, J. Med. Chem. 59 (2016) 4539–4550.
[23] T. Tsukamoto, K.M. Wozniak, B.S. Slusher, Progress in the discovery and development of glutamate carboxypeptidase II inhibitors, Drug Discov. Today 12 (2007) 767–776.
[24] C. Zhong, X. Zhao, J. Sarva, A. Kozikowski, J.H. Neale, B.G. Lyeth, NAAG peptidase inhibitor reduces acute neuronal degeneration and astrocyte damage following lateral fluid percussion TBI in rats, J. Neurotrauma 22 (2005) 266–276.
[25] T. Yamamoto, S. Hirasawa, B. Wroblewska, E. Grajkowska, J. Zhou, A. Kozikowski, J. Wroblewski, J.H. Neale, Antinociceptive effects of N-acetylaspartylglutamate (NAAG) peptidase inhibitors ZJ-11, ZJ-17 and ZJ-43 in the rat formalin test and in the rat neuropathic pain model, Eur. J. Neurosci. 20 (2004) 483–494.
[26] H. Wang, Y. Byun, C. Barinka, M. Pullambhatla, H.E. Bhang, J.J. Fox, J. Lubkowski, R.C. Mease, M.G. Pomper, Bioisosterism of urea-based GCPII inhibitors: Synthesis and structure-activity relationship studies, Bioorg. Med. Chem. Lett. 20 (2010) 392–397.
[27] A.P. Kozikowski, J. Zhang, F. Nan, P.A. Petukhov, E. Grajkowska, J.T. Wroblewski, T. Yamamoto, T. Bzdega, B. Wroblewska, J.H. Neale, Synthesis of urea-based inhibitors as active site probes of glutamate carboxypeptidase II: efficacy as analgesic agents, J. Med. Chem. 47 (2004) 1729–1738.
[28] Y. Chen, C.A. Foss, Y. Byun, S. Nimmagadda, M. Pullambhatla, J.J. Fox, M. Castanares, S.E. Lupold, J.W. Babich, R.C. Mease, M.G. Pomper, Radiohalogenated prostate-specific membrane antigen (PSMA)-based ureas as imaging agents for prostate cancer, J. Med. Chem. 51 (2008) 7933–7943.
[29] S.H. Son, H. Kwon, H.H. Ahn, H. Nam, K. Kim, S. Nam, D. Choi, H. Ha, I. Minn, Y. Byun, Design and synthesis of a novel BODIPY-labeled PSMA inhibitor, Bioorg. Med. Chem. Lett. 30 (2020), 126894.
[30] H. Kwon, S.H. Son, Y. Byun, Prostate-Specific Membrane Antigen (PSMA)-Targeted Radionuclide Probes for Imaging and Therapy of Prostate Cancer, Asian J. Org. Chem. 8 (2019) 1588–1600.
[31] D.V. Ferraris, K. Shukla, T. Tsukamoto, Structure-activity relationships of glutamate carboxypeptidase II (GCPII) inhibitors, Curr. Med. Chem. 19 (2012) 1282–1294.
[32] A.X. Zhang, R.P. Murelli, C. Barinka, J. Michel, A. Cocleaza, W.L. Jorgensen, J. Lubkowski, D.A. Spiegel, A remote arene-binding site on prostate specific membrane antigen revealed by antibody-recruiting small molecules, J. Am. Chem. Soc. 132 (2010) 12711–12716.
[33] S.R. Banerjee, C.A. Foss, M. Castanares, R.C. Mease, Y. Byun, J.J. Fox, J. Hilton, S. E. Lupold, A.P. Kozikowski, M.G. Pomper, Synthesis and evaluation of technetium-99m- and rhenium-labeled inhibitors of the prostate-specific membrane antigen (PSMA), J. Med. Chem. 51 (2008) 4504–4517.
[34] S.P. Rowe, M.A. Gorin, M.G. Pomper, Imaging of Prostate-Specific Membrane Antigen with Small-Molecule PET Radiotracers: From the Bench to Advanced Clinical Applications, Annu. Rev. Med. 70 (2019) 461–477.
[35] C. Kratochwil, A. Afshar-Oromieh, K. Kopka, U. Haberkorn, F.L. Giesel, Current Status of Prostate-Specific Membrane Antigen Targeting in Nuclear Medicine: Clinical Translation of Chelator Containing Prostate-Specific Membrane Antigen Ligands Into Diagnostics and Therapy for Prostate Cancer, Semin. Nucl. Med. 46 (2016) 405–418.
[36] K. Kim, H. Kwon, C. Barinka, L. Motlova, S. Nam, D. Choi, H. Ha, H. Nam, S.H. Son, I. Minn, M.G. Pomper, X. Yang, Z. Kutil, Y. Byun, Novel β- and γ-Amino Acid-Derived Inhibitors of Prostate-Specific Membrane Antigen, J. Med. Chem. 63 (2020) 3261–3273.
[37] C. Barinka, Z. Novakova, N. Hin, D. Bim, D.V. Ferraris, B. Duvall, G. Kabarriti, R. Tsukamoto, M. Budesinsky, L. Motlova, C. Rojas, B.S. Slusher, T.A. Rokob, L. Rulisek, T. Tsukamoto, Structural and computational basis for potent inhibition of glutamate carboxypeptidase II by carbamate-based inhibitors, Bioorg. Med. Chem. 27 (2019) 255–264.
[38] M.B. Robinson, R.D. Blakely, R. Couto, J.T. Coyle, Hydrolysis of the brain dipeptide N-acetyl-L-aspartyl-L-glutamate. Identification and characterization of a novel N-acetylated alpha-linked acidic dipeptidase activity from rat brain, J. Biol. Chem. 262 (1987) 14498–14506.
[39] S.R. Banerjee, M. Pullambhatla, Y. Byun, S. Nimmagadda, C.A. Foss, G. Green, J. J. Fox, S.E. Lupold, R.C. Mease, M.G. Pomper, Sequential SPECT and optical imaging of experimental models of prostate cancer with a dual modality inhibitor of the prostate-specific membrane antigen, Angew. Chem. Int. Ed. Engl. 50 (2011) 9167–9170.
[40] J. Tykvart, J. Schimer, J. Barinkova, P. Pachl, L. Postova-Slavetinska, P. Majer, J. Konvalinka, P. Sacha, Rational design of urea-based glutamate carboxypeptidase II (GCPII) inhibitors as versatile tools for specific drug targeting and delivery, Bioorg. Med. Chem. 22 (2014) 4099–4108.
[41] R. Nakajima, Z. Novakova, W. Tueckmantel, L. Motlova, C. Barinka, A. P. Kozikowski, 2-Aminoadipic Acid-C(O)-Glutamate Based Prostate-Specific Membrane Antigen Ligands for Potential Use as Theranostics, ACS Med. Chem. Lett. 9 (2018) 1099–1104.
[42] J. Tykvart, J. Schimer, A. Jancarik, J. Barinkova, V. Navratil, J. Starkova, K. Sramkova, J. Konvalinka, P. Majer, P. Sacha, Design of highly potent urea-based, exosite-binding inhibitors selective for glutamate carboxypeptidase II, J. Med. Chem. 58 (2015) 4357–4363.
[43] A.J. Oliver, O. Wiest, P. Helquist, M.J. Miller, M. Tenniswood, Conformational and SAR analysis of NAALADase and PSMA inhibitors, Bioorg. Med. Chem. 11 (2003) 4455–4461.
[44] X. Duan, F. Liu, H. Kwon, Y. Byun, I. Minn, X. Cai, J. Zhang, M.G. Pomper, Z. Yang, Z. Xi, X. Yang, (S)-3-(Carboxyformamido)-2-(3-(carboxymethyl)ureido)propanoic Acid as a Novel PSMA Targeting Scaffold for Prostate Cancer Imaging, J. Med. Chem. 63 (2020) 3563–3576.
[45] L.A. Khawli, A.I. Kassis, Synthesis of 125I labeled N-succinimidyl p-iodobenzoate for use in radiolabeling antibodies, Int. J. Rad. Appl. Instrum. B 16 (1989) 727–733.